Electronic Supplementary Material (ESI) for Faraday Discussions.
This journal is © The Royal Society of Chemistry 2018



Supplementary Information for:

# Systematic Control of the Rate of Singlet Fission within 6,13-Diphenylpentacene Aggregates with PbS Quantum Dot Templates

*Chen Wang[†], Mohamad S. Kodaimati[‡], Shichen Lian[‡] and Emily A. Weiss[‡]**

*[†] Department of Chemistry and Biochemistry, City University of New York, Queens College, 65-30 Kissena Blvd., Flushing, NY, 11367*

*[‡] Department of Chemistry, Northwestern University, 2145 Sheridan Rd., Evanston, IL 60208-3113*

*corresponding author. Email: e-weiss@northwestern.edu

Table of Contents

## 1. DLS results of DPP-QD coaggregates

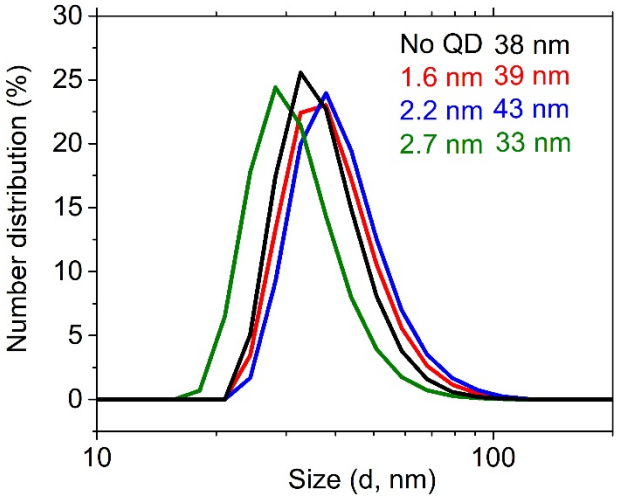


**Figure S1** Particle size analysis for DPP and DPP-QD aggregates with DLS.

## 2. TA spectra and kinetics of DPP aggregates

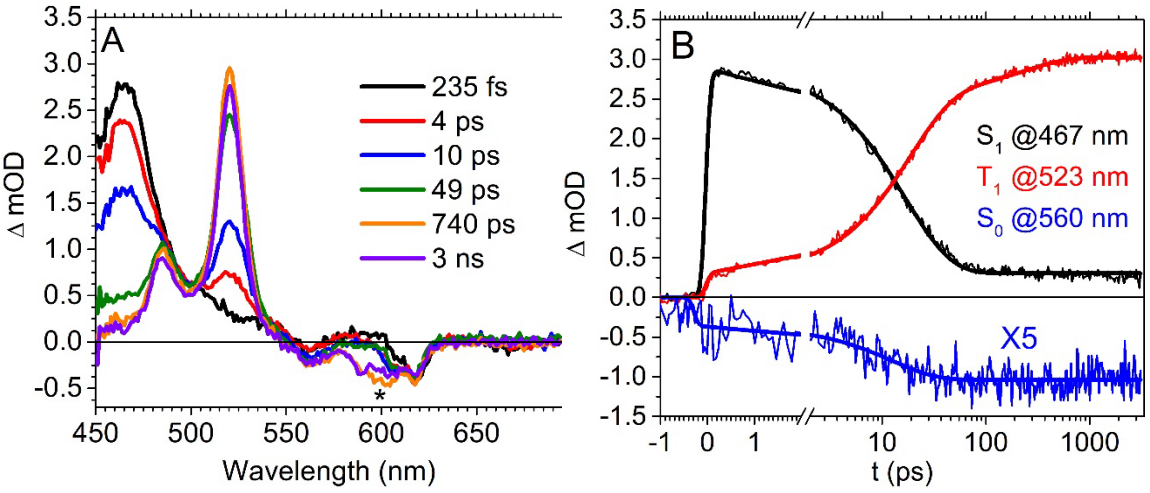


**Figure S2. (A)** Selected fs-TA spectra of the DPP aggregates at a series of time delays after excitation at 610 nm. The asterisk indicates the spectral region affected by pump scatter. **(B)** Kinetic traces extracted from the TA spectra in (A) at 467 nm (the $S_1$ absorption), 523 nm (the $T_1$ absorption) and the 560 nm (the $S_0$ bleach). It is worthwhile to note that the bleach signal appears with a time constant of 14 ps, synchronous with the decay of the $S_1$ signal and the growth of the $T_1$ signal. This result is characteristic of the singlet fission process, which converts one more ground state molecules to the triplet excited state upon photoexcitation.

**3. TA spectra and kinetics of QD/DPP coaggregates with 970 nm excitations**

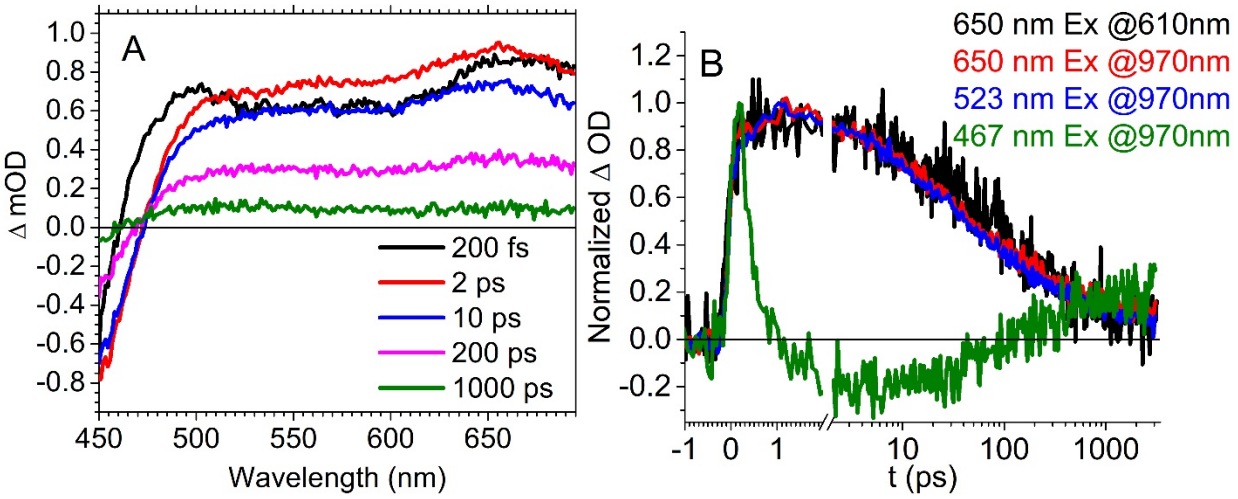


**Figure S3. (A)** Selected fs-TA spectra of the DPP/QD (r =2.2 nm) aggregates at a series of time delays after excitation at 970 nm. **(B)** Normalized kinetic traces extracted from Main Text **Figure 3 (A)** at 650 nm, after photoexcitation 610 nm, and from **Figure S2(A)** at 650 nm, 523 nm and 467 nm, after excitation at 970 nm.

The decay of PIA of the QDs is independent of the excitation wavelength. The PIA signal decays at the same rate across the 500-700 nm region. However, at 467 nm, the kinetics are dominated by a positive feature associated with the unrelaxed exciton, which quickly disappears. After a 1-ps time delay, the 467 nm region behaves as a pseudo-isosbestic point.

**4. Removing the PbS PIA background from the TA kinetics of DPP within DPP/QD coaggregates.**

By comparing the PIA intensities at 650 nm, where there is no overlapping DPP signal, for TA spectra collected with 610 and 970 nm excitation, we determined that the spectra obtained with 970-nm photoexcitation must be scaled by a factor of 2.6 before being subtracted from spectra obtained with 610-nm photoexcitation. We subtracted these scaled signals at corresponding wavelengths from the raw kinetic traces collected with 610 nm excitation to obtain the pure kinetics of DPP aggregates within assemblies with QDs (**Figure S4**).

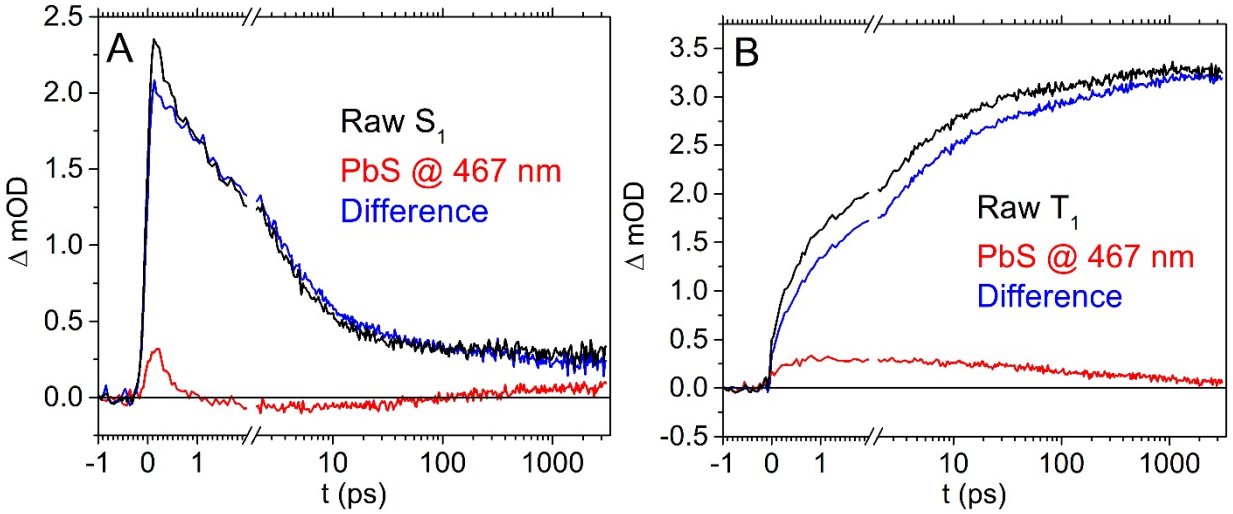


**Figure S4.** Subtraction of the scaled kinetic traces at **(A)** 467 nm and **(B)** 523 nm obtained with 970-nm excitation from the raw data collected with 610-nm excitation to obtain the pure kinetics of the $S_1$ and $T_1$ states of DPP within the DPP/QD co-aggregates.

**5. DADS Analysis for the TA Data of DPP/QD Co-aggregates**

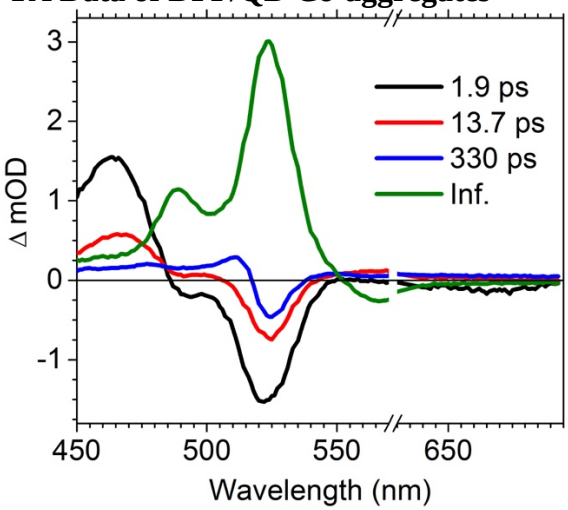


**Figure S5.** Decay associated difference spectra analysis for the singlet fission process of DPP co-aggregated with PbS QDs with r = 2.2 nm. The PIA of the QDs has been removed before analysis by subtracting the transient background of QDs.

The decay associated difference spectra (DADS) were obtained for the singlet fission process within DPP co-aggregated with 2.2-nm QDs (Figure S5). The analysis was based on the kinetic model shown in Eq. 1 of the main text, and carried out using the SufaceXplorer software. The spectral feature with a 1.9 ps decay lifetime is associated with the fast singlet fission process, and the 13.7 ps species corresponds to the slower singlet fission process. The differential-like feature with a decay lifetime of 330 ps represents the change of the spectral feature from $(T_1T_1)^1$ to $(T_1\ldots\ldots T_1)$, which involves a decrease of absorption intensity in the 450-510 nm region and a growth at ~525 nm.

**6. Comparison of hole transfer within the co-aggregates of PbS QDs with r=1.6 and 2.2 nm.**

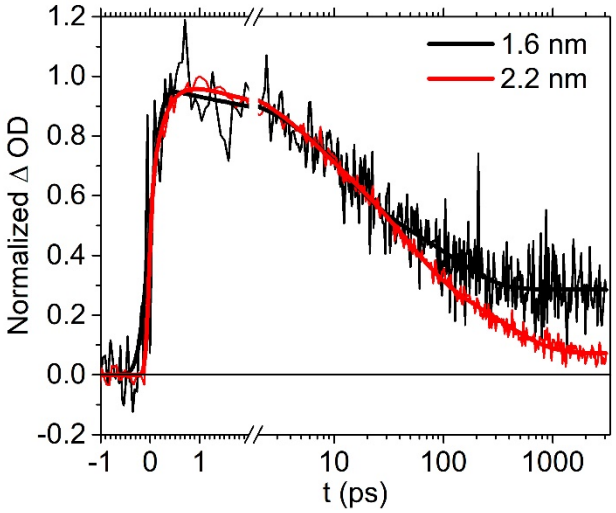


**Figure S6.** The comparison of normalized kinetic traces of the QD PIA at 650 nm for QDs with radii of 1.6 and 2.2 nm.

The decays in **Figure S6** are fit with three exponential components as listed in **Table S1**. The average decay time constant is 26 ps for r = 1.6 nm, and is 18 ps for r = 2.2 nm QDs. The faster decay of the QD shelf signal for r = 2.2 nm QDs indicates a faster hole transfer from QD to DPP, which suggests that DPP is closer to the QD surface for r = 2.2 nm than for r = 1.6 nm.

**Table S1.** Exponential fitting parameters for the decay kinetic traces in **Figure S6**

| QD Radius (nm) | $\tau_1$, ps (Amp. %) | $\tau_1$, ps (Amp. %) | $\tau_1$, ps (Amp. %) | $\tau_{avg}$, ps |
|---|---|---|---|---|
| 1.6 nm | 11 (39) | 120 (29) | 1200 (32) | 26 |
| 2.2 nm | 5 (24) | 40 (27) | 360 (49) | 18 |

## 7. Quantification of the ligand density of PEGT on PbS QDs

We applied $^{1}H$ NMR to quantify the number of bound PEGT ligands per QD using dimethyl sulfoxide as the internal integration standard. First, we measured the NMR spectrum of a sample with 10 mg of PEGT (M.W.=1000) and 20 eq. DMSO dissolved in 0.8 ml $D_2O$, and determined a ratio of the integration areas eq. PEGT:eq DMSO = 14.7:1. Second, QDs in $D_2O$ with known concentrations were measured with DMSO as internal standard, to calculate the numbers of PEGT ligands per QD in each sample. Last, the densities of PEGT ligands were obtained by dividing the number of PEGT ligands by the surface areas of the QDs, treating them as spheres. The results are listed in **Table S2**.

**Table S2.** Quantification of the densities of PEGT ligands on QDs of different radii, r.

| r(QDs) (nm) | $C_{PETG}$ (mM) | $C_{QDs}$ (μM) | PEGT/QD | Density /$nm^2$ |
|---|---|---|---|---|
| 2.7 | 2.18 | 12.70 | 172 | 1.9 |
| 2.4 | 1.23 | 7.64 | 161 | 2.2 |
| 2.2 | 1.16 | 7.63 | 152 | 2.5 |
| 2.0 | 1.88 | 13.00 | 144 | 2.9 |
| 1.8 | 1.40 | 10.50 | 133 | 3.3 |
| 1.6 | 1.41 | 12.30 | 114 | 3.6 |